

Manufacturing sector: Cement

Badr Ben m'barek¹, Mason Phillipott¹ and Clément De Daniloff^a

¹⁾ TransitionZero



1. Introduction

There is one important number that encapsulates the tremendous importance of the cement industry worldwide: 7%. It describes both the global industrial energy use of the cement sector, making it the third-largest industrial energy consumer, but it also captures the fraction of global carbon dioxide (CO₂) emissions for whom this sector is responsible for (IEA, 2018). Thus, it has the second-largest share of total direct industrial CO₂ emissions. The majority of emissions related to the cement industry do not originate from the large quantities of thermal energy that are provided from fossil fuels combustion but are rather due to the calcination process directly. In 2016, global process emissions from cement production were equivalent to about 4% of global emissions from fossil fuels (Andrew, 2018). Mixed with air, water, sand and gravel, cement makes concrete, the most consumed manufactured substance on the planet. Concrete builds homes, schools, hospitals, workplaces, transport systems and infrastructure for clean water, sanitation and energy, which are essential for quality of life as well as social and economic wellbeing. Due to the key role it plays in modern society, cement demand is expected to grow by 12-23% by 2050 from 2018 levels (IEA, 2018). Whereas the rest of the global cement production is widely spread around the globe, almost three quarters of it originates from only two countries: China accounts for almost 60% of global production, and India is responsible for 16% (IEA, 2018).

Most importantly, cement production can be used as a proxy for emissions and therefore it is desirable to ascertain real time and in-depth production values to guide future climate policy. With any such globally traded commodity, however, it is characterised by fierce competition amongst producers and, consequently, facility level production data is rarely made publicly available. In most cases, it is only possible to obtain cement production and emissions quantities at the country level, and often there is a substantial delay (~years) in obtaining the data (GNR contributors, 2020).

In this work, we address both the temporal and spatial limitations in traditional cement emissions reporting to provide more timely and accurate facility level data. More specifically, we have aimed to deliver cement emissions based on clinker production estimates on a monthly basis (with 2 to 4 months lag depending on data availability) for all assets identified on the Spatial

Finance Initiative database (McCarten et al., 2021; see also Section 2.1.1). Our approach improves upon certain capacity-based approaches which may only proportionately infer production between facilities or assign some average utilisation rates of installed capacities. The approach achieves this using satellite-derived mapping data which can capture variation in activity for most clinker-producing cement facilities - and use this data to infer clinker production in a given time frame.

2. Materials and Methods

To produce cement, direct emissions are released during the manufacturing of clinker, not only because of the CO₂ generated in the calcination chemical reaction, but also because of the combustion of fossil fuels which provides most of thermal energy. More information on cement production is provided in section 7.1 and highlighted in Figure 7.

By using a combination of satellite imagery, publicly reported data and academic papers, we estimate the production of clinker and infer the corresponding emissions of the cement sector. This section provides a high-level overview of the datasets and associated pipelines used to achieve that goal.

Given the lack of asset-level emission data publicly available, a standardised “bottom-up” approach is used to quantify the emissions. This process is characterised by first estimating production levels for each plant in tons of clinker before then subsequently applying a calculated emission factor (tons of CO₂ per ton of clinker produced) to generate emissions estimates.

There are primarily two approaches to estimating asset level production. As a priority, satellite-derived production estimates are used whenever a facility releases enough heat to be captured by satellite imagery (Zhou *et al.*, 2018; Marchese *et al.*, 2019; Liangrocapart, Khetkeeree and Petchthaweeetham, 2020). This is the case for clinker-producing plants as clinkerization occurs for high temperatures of around 1,400°C. For plants where no suitable hotspot signals were found (see Section 7.3), we used a basic disaggregation method. This is determined by calculating each plant's share of national capacity, before multiplying this number by the country's production to derive the plant's contribution for the given timeframe. For country-level statistics these point-source estimates are then aggregated. Figure 1 summarises the modelling approach, however, M'Barek and Gray, (2021) provide a more detailed methodological breakdown.

2.1. Materials

2.1.1. Asset inventory dataset

Cement production consists of three steps: first limestone is mixed with other materials, then the mixture is heated up to produce clinker, and finally this clinker is grinded together with other ingredients to produce cement. The final grinding process can happen in so-called integrated facilities where the clinker is also produced or in independent grinding facilities closer to its end market. Spatial Finance Initiative provides facility level information such as GPS coordinates, owner, capacity, age, product type and technology type (McCarten et al., 2021). The database includes both integrated and grinding plant types. In this work, we estimate cement emissions based on clinker production and therefore we only keep integrated plants. We include plants corresponding to entries where the plant type is unspecified when it is possible to identify them as clinker-producing plants. In total there are 2,267 cement plants across 137 countries. We manually validated the position of all the plants using geolocation data from Google Maps API (Google Maps, 2022) and OpenStreetMap (OpenStreetMap, 2022).

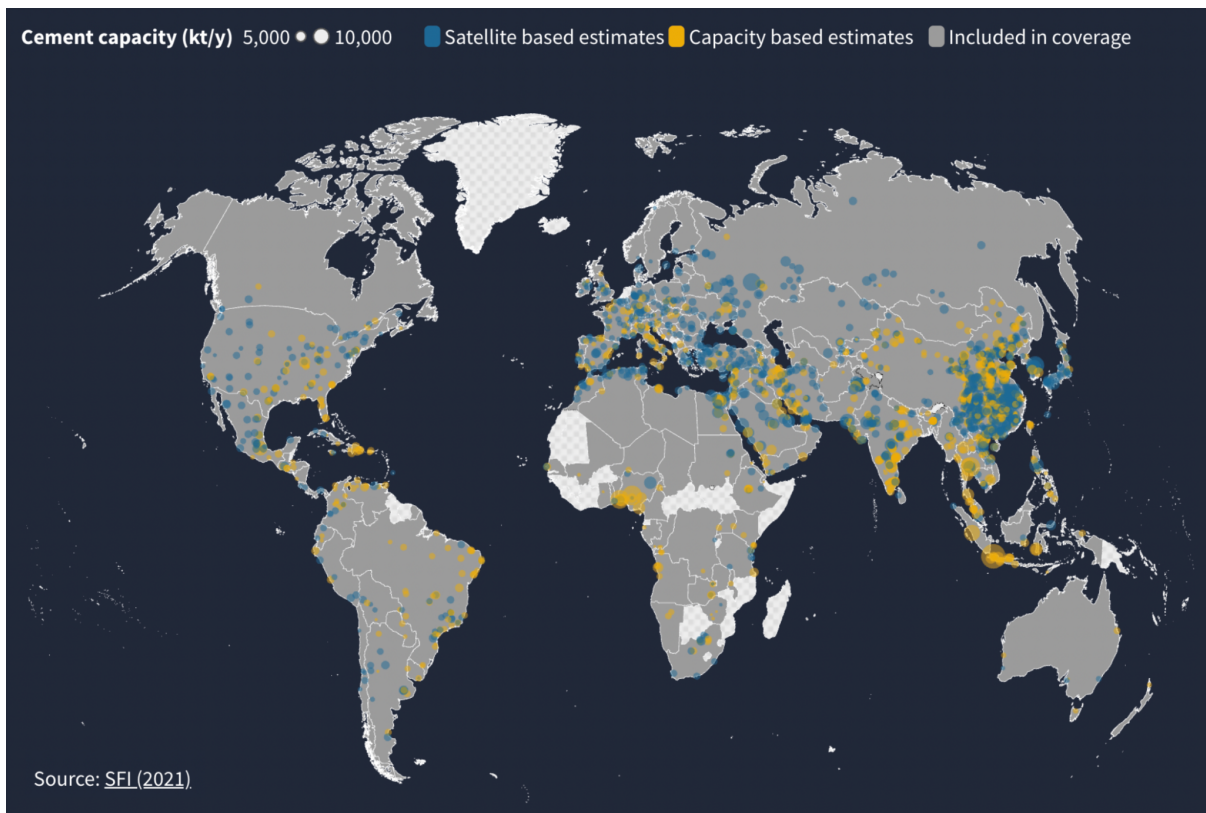


Figure 1 Global map showing integrated cement facilities. Countries included in cement emissions monitoring are shaded. Assets that are monitored with satellites are shown in blue, whereas others where a capacity-based estimate is used to infer their production are shown in orange. Source: McCarten et al. (2021).

Figure 1 shows how clinker-producing assets are distributed globally with high concentration of assets in China which produces more than half of the global production, followed by India at 16% (facility count details in Section 7.4). The map also highlights countries with little to no clinker production.

2.1.2. Remote sensing datasets

Satellite-based production estimates make use of multispectral image from two different collections:

- The European Space Agency (ESA) Copernicus Sentinel mission with a resolution of 20m and a combined 5-day at the equator revisit with two satellites:
 - Sentinel 2A: with historical images available since 2017 (ESA, 2022).
 - Sentinel 2B: with historical images available since 2017 (ESA, 2022).
- The U.S. Geological Survey (USGS) and National Aeronautics and Space Administration (NASA) Landsat program with a resolution of 30m and a combined 8-day revisit:
 - Landsat-8: with historical images available since 2015 (NASA and USGS, 2022a).
 - Landsat-9: with historical images available from 2022 (NASA and USGS, 2022b).

All images are sourced and processed using Google Earth Engine (Google Earth Engine, 2022a, 2022b, 2022c). For each image, we rely on the surface reflectance product and compute the normalised band ratio between the two short wave infrared bands of each satellite, called the Normalised Heat Index (NHI). For the respective satellite collections, we infer the NHI through the following calculations:

- Sentinel-2A/B: $NHI = \frac{(B12 - B11)}{(B12 + B11)}$
- Landsat-8/9: $NHI = \frac{(B07 - B06)}{(B07 + B06)}$

Where B# refers to the band number for the specific satellite. This ratio is used to identify thermal anomalies within the temperature range of industrial processes, while eliminating most of the noise from reflectance interference (adapted from Kato, (2021) for industrial applications). Pixel values between the Sentinel 2A/B MultiSpectral Instrument and Landsat Operational Land Imager Instrument were harmonised using NASA's band pass adjustments (NASA, 2018), allowing the two image collections to be used as if they were a single collection. The harmonised dataset ensured higher revisit for time-series surface applications. Partial images (coverage of the facility's boundaries less than 80%) and cloudy images (more than 20% clouds) are excluded. Figure 2 shows an example of NHI with identified hotspot locations at a cement plant.



Figure 2 Left - high resolution image from August 2019 of Roberta Cement Plant (U.S.A), overlaid with manual labelling of the two visible rotary kilns where large amounts of heat are released for clinkerization to occur. Middle - composite Sentinel-2 image acquired on November 8th, 2021, using the NHI which shows thermal anomalies (red for hot pixels, blue for cooler pixels); Right - composite Landsat 8/9 image acquired the same day, also using the NHI to show thermal anomalies. Sources: modified Copernicus and USGS data, and Terrametrics.

2.1.3. Production datasets

Cement production emissions are closely associated with the volume of clinker produced (Andrew, 2019). As such, our target data was that of clinker production. With lacking freely and widely available clinker production data we look to approximate production estimates through the more widely available cement production, using the most relevant/accurate data source for each country. To perform these estimates, data from the following sources were employed:

- Countries reported monthly cement production for the United States (at state level), China (at province level), and Japan (at country level),
- Monthly cement production data for the 36 countries from the Monthly Bulletin of Statistics Online (MBS, 2022),
- Monthly non-metallic mineral production index data for the 68 countries available countries from the United Nations Industrial Development Organization data sets (UNIDO, 2022),
- Annual cement production available for almost all geographies through the United States Geological Survey data sets (USGS, 2022),
- Monthly clinker imports from the United Nations Comtrade database (UN Comtrade, 2022).

Each of these datasets was used to develop four models to estimate cement production. The detailed methodology of these estimates and model development is presented in section 7.1.

2.1.4. Emissions factors dataset

A global emission factor was used for cement process emissions (IPCC, 2006). Emissions related to the direct or indirect use of fuel were estimated using both data from the Getting the Number Right (GNR) datasets and local power grid intensities from the International Energy Agency (IEA, 2020). The GNR database provides data which allows us to estimate emission factors (except for process emissions) at country level (18 countries), and geographical region level (9 regions). Countries include Algeria, Austria, Brazil, Canada, Czech Republic, Egypt, France, Germany, India, Italy, Morocco, Philippines, Poland, Spain, Thailand, Tunisia, United Kingdom, United States. Geographical regions include Africa, Commonwealth of Independent States, Central America, Europe, Middle East, North America, Northeast Asia, South America (except Brazil) and Other Asian countries + Oceania. The countries not listed above are mapped to their corresponding geographical region, when possible, otherwise they are assigned the world-averaged emission factors.

2.1.5. Validation datasets

Facility level production and emissions models were developed based upon country-level target data. As a consequence, alternative sources were required to validate our model results. Our results were validated against reported emissions. Globally, only the US Environmental Protection Agency (US EPA) and the European Pollutant Release and Transfer Register (E-PRTR) published facility level data (E-PRTR contributors, 2022; US EPA contributors, 2022). In this work, both sets of these values were recorded on an annual basis and were utilised as a benchmark to validate the performance of our own model estimates.

2.2. Methods

In this work, cement sector emissions were estimated by first monitoring the clinker production then applying emissions factors to infer CO₂ emissions. Thus, cement plants that perform grinding and blending exclusively were excluded. In the next sections, details on the methods used to infer production and to model emissions are provided.

2.2.1. Production methodology

2.2.1.1. Satellite based estimates

Integrated cement plants produce clinker in large kilns that can be resolved in satellite images. Hotspot activities from these kilns were identified from the satellite NHIs, country level production data was used to calibrate the relationships between these activities and production at the plant level, visualised in Figure 3. Specifically, we begin by extracting the shapes of all hotspots at each plant. For each of these hotspots, a time-series of pixel values was extracted before signal processing was applied to normalise these values between zero and one. Each normalised hotspot time-series was fed into an optimizer function which developed a linear

relationship (or weight) between hotspot NHI and reported country level production. Model constraints were also implemented during this optimization phase that ensured individual plant predictions should not exceed their maximum capacity. The asset production estimates were then back calculated using the asset's hotspot signals and their corresponding weight.

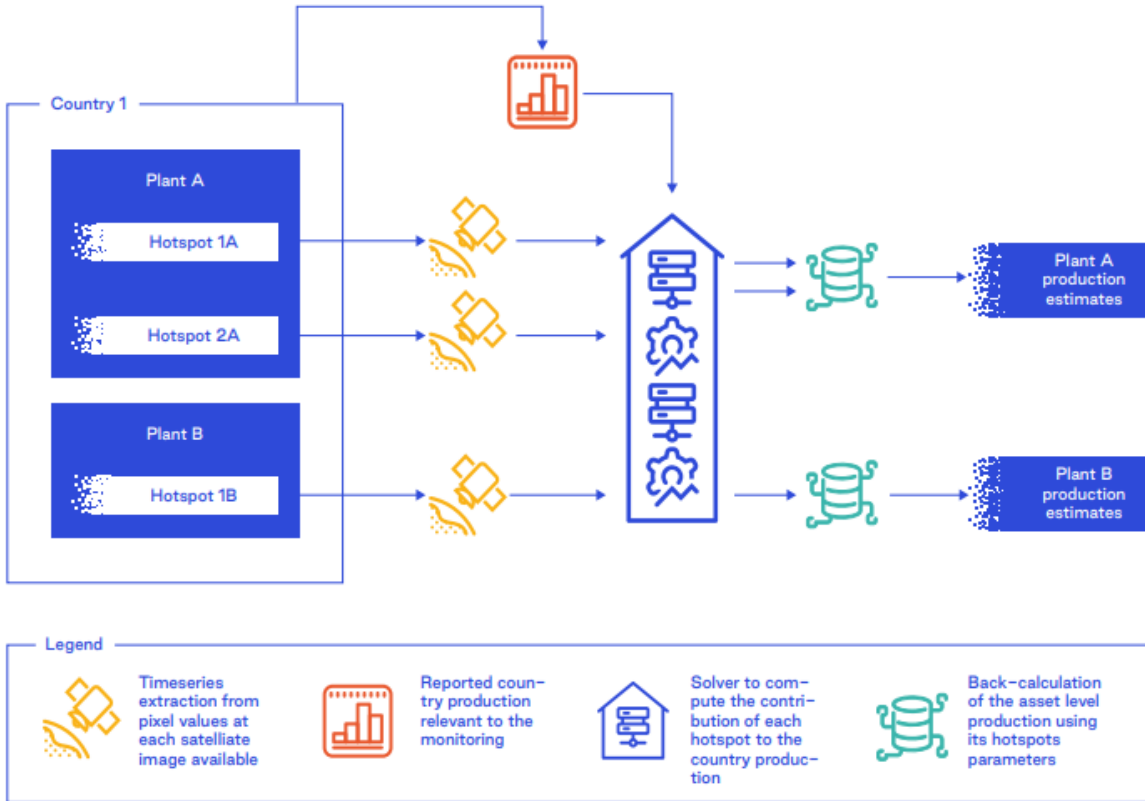


Figure 3 Schematic model approach for satellite-based estimates of facility level production.

2.2.1.2. Capacity based estimates

For assets which are not monitored via satellite (see Section 4), a basic disaggregation method was applied: for each facility, its share of national capacity was computed, before multiplying this number by the country's remaining production (after accounting for satellite-derived asset production estimates) to derive the facility's contribution for the given timeframe. An illustrative example of a country with two plants A and B (of capacities C_A and C_B respectively) and a total production P_m for a country/region and a given month m , the capacity-based estimates for these two plants are (respectively $P_{A,m}$ and $P_{B,m}$):

- $P_{A,m} = \frac{C_A}{C_A + C_B} \times P_m$
- $P_{B,m} = \frac{C_B}{C_A + C_B} \times P_m$

2.2.1.3. Non-spatially allocated asset estimates

In some cases, there is a shortfall between the sum of satellite and capacity-based asset production estimates and the country-level production targets. This circumstance may occur when the capacity of listed assets is lower than the aggregated production figures (country or province-level). This missing production is then allocated to a non-spatially allocated asset for the purposes of more accurately estimating country-level emissions.

2.2.2. Emissions methodology

We model emissions by multiplying clinker production by emission factors including different types of emissions. We detail in this section the different emissions factors considered and their corresponding source. Two types of emissions are accounted for here: direct and indirect emissions. Direct emissions were split into process emissions and fuel emissions. Fuel emissions were further split into kiln fuel and non-kiln fuel emissions. Table 1 gives a summary of the emission model used in this work, and Figure 4 shows emission breakdowns for wet and dry processes by category. The GNR project contains yearly data up to 2019 in the current version. Depending on the country or region and the table of interest, some years might be missing. Emission factors dependent on GNR numbers were only estimated for 2012 and later, where we found the data availability to be acceptable. Missing years were interpolated linearly prior to the most recent available year and extrapolated with a forward fill for those years after. More details about the emission types are provided below.

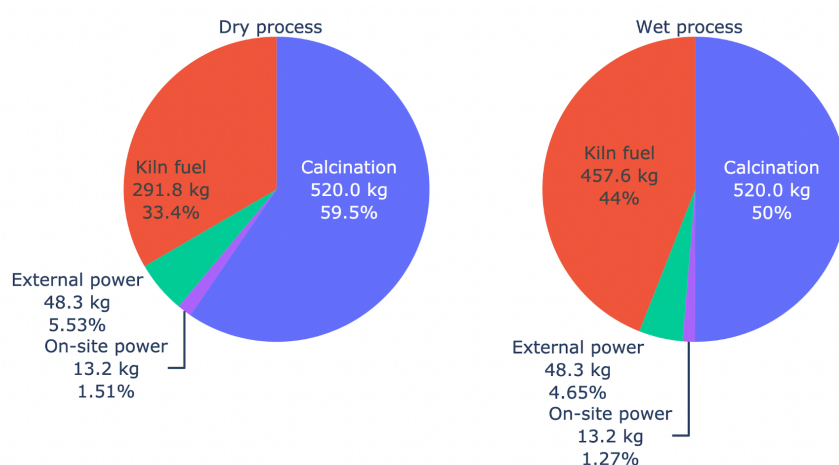


Figure 4 Global emissions factors breakdown for cement manufacturing in 2019 for dry and wet processes. The values are expressed in kg CO₂ / tons of clinker. Despite that, external power includes the energy required for the further cement grinding process.

Table 1 Summary of the emission model.

Type of emissions	Direct emissions			Indirect emissions External power consumption from the national grid	
	<i>Process emissions</i>	<i>Fuel emissions</i>			
	Limestone calcination $\text{CaCO}_3 \rightarrow \text{CaCO} + \text{CO}_2$ Cement kiln dust	Kiln fuel emissions	Non-kiln fuel emissions		
Source	IPCC EFDB ID: 213926	GNR	GNR	GNR and IEA	
Scope	Global	Country or geographical region Corrected for kiln type (wet or dry) depending on information availability	Country or geographical region	Country or geographical region	

Process emissions: A constant and global factor of 520 kg CO₂ / tons of clinker was applied to account for process emissions. This emission factor originates from the Emission Factor Database (EFDB) used by the Intergovernmental Panel on Climate Change (ID: 213926; <https://www.ipcc-nrgip.iges.or.jp/EFDB/main.php>) and describes the emissions due to the limestone calcination process CaCO₃ → CaCO + CO₂, assuming a CaO content of 65% for clinker and applying a 2% correction factor for cement kiln dust. Emissions from the MgCO₃ → MgCO + CO₂ process were neglected due to the small fraction of magnesium in the clinker.

Kiln-fuel emissions: The definition of kiln-fuel emissions used here matches the Cement CO₂ Protocol used to collect the GNR data. These emissions include the heat consumption of kilns, but also the heat used for drying fuels and raw materials. In this work, we obtained the corresponding emission factor at country- or region-level by multiplying the thermal energy consumption per ton of clinker by the carbon intensity of the fuel mix. The latter only included emissions from fossil-based fuels (conventional and alternative), omitting emissions from biomass-based fuels combustion (even when they are mixed with fossil fuels).

Non-kiln fuel emissions: Non-kiln fuel emissions from on-site power generation were estimated. The total energy created in the form of electricity reported in GNR data was converted

into primary energy by assuming a thermal-to-electric efficiency of 33%. Then, the result was multiplied by the carbon intensity of the fuel mix (assumed to be identical to the one of the kiln fuel mix, available in GNR data) and divided by the production volume of clinker to get the corresponding emission factor. Other non-kiln fuel emissions defined in the Cement CO₂ Protocol (on-site equipment, on-site vehicles, room heating/cooling and the drying of mineral components) were not accounted for in this work. By using the directly reported gross CO₂ emissions from GNR and subtracting the estimated emissions from usages other than non-kiln fuel combustion, non-kiln fuels typically contribute to ~2% of the cement emissions worldwide. Locally, the share of non-kiln fuel emissions ranges from <1% to 5%.

Indirect emissions: The indirect emissions that were accounted for originate from the external power consumption. They were obtained by multiplying the amount of energy supplied by the local national grid with the associated grid carbon intensity. The former was obtained from the GNR data at country- or region-level, whereas the latter was obtained from the IEA data at the country level. For regional data, the weighted-average grid intensity was calculated using the total production of each country within the region.

Correction for kiln type: The thermal energy consumption of kilns depends significantly on the production type of a given plant. There are two basic types of clinker production – “wet” or “dry” – depending on the moisture content of raw materials, and there are also different kiln designs. The wet process consumes more energy than the dry process, as the moisture needs to evaporate (IEA, 2018). For most entries, the asset database specifies whether plants use a dry or a wet process. The shares of reported assets using dry, wet and unspecified process types are 92%, 3% and 5%, respectively. When available, this information allowed us to apply a correction to the kiln fuel emission factor of a given plant. The GNR data contains tables that distinguished between different kiln types among the following categories: wet/shaft kiln, dry with preheater and precalciner, dry with preheater without precalciner, dry without preheater (long dry kiln), semi-wet/semi-dry. Due to confidentiality reasons, an additional category “mixed kiln type” contains all the aggregated data from assets whose production type was not publicly available, which was discarded in the following. Because of poor GNR data availability at country and region levels, global correction factors were inferred for each available year using exclusively world data, which were then applied to locally estimated kiln fuel emission factors. Using the correction factors, two emission factors were obtained for kiln fuels associated with wet and dry processes, such that their ratio is equal to the reported world weighted-average ratio, and such that their weighted-average reproduces the asset uncorrected emission factor. The weighting was performed by clinker production volumes, and GNR production types were related to wet or dry type as indicated in Table 2. If the production type is unavailable, the uncorrected emission factor is used.

Table 2 Mapping to wet and dry processes from GNR dataset plant types.

Available GNR data types	Asset data type
Wet / Shaft kiln	Wet
Dry with preheater and precalciner Dry with preheater without precalciner Dry without preheater (long dry kiln) Semi-wet/semi-dry	Dry

2.3. Coverage

Based on 2021 production numbers, asset level estimates for 75% (2,306 Mt/a) of world clinker production were provided. The remaining 25% were provided through the country level estimates as non-spatially allocated assets. Satellite-monitored assets represented 52% of total assets (1178 out of 2256), these assets contributed to 54% of the total asset level cement emissions estimates (1,097 out of 2,022 MtCO₂/a) in 2021. A more detailed breakdown of coverage is available in Section 7.4.

3. Results and analysis

Our methodology provides production and, by extension, emissions estimates at a monthly level. In this section, our results are provided through statistical analysis. Accuracy is assessed by first gathering production and emissions data for assets before then subsequently calculating median of absolute errors (MAE) and median of absolute percentage errors (MAPE) statistics across data. The results section consists of the following subsections that explore how our modelled emissions estimates compare to external sources: plant level cement emissions (Section 3.2), and aggregated cement emissions (Section 3.4).

3.1. Comparison of asset level emissions estimates

In this section our CO₂ emissions estimates are compared to reported data by the US EPA and E-PRTR (US EPA, 2022; E-PRTR, 2022). Data is published at an annual resolution in both cases, so our own monthly emissions estimates will be aggregated on an annual basis for comparison. The results of this analysis are displayed in Figure 5. In total there are 214 assets (1122 samples) of which 123 are from the EU (579 samples) and 91 from the US (543 samples). Overall, MAE (MAPE) accuracy across the samples is 0.21 MtCO₂/a (33%). Of the 214 assets, 75 are capacity based (398 samples) and 139 are satellite-based (724 samples) with accuracy of 0.20 MtCO₂/a (31%) and 0.22 MtCO₂/a (33%), respectively.

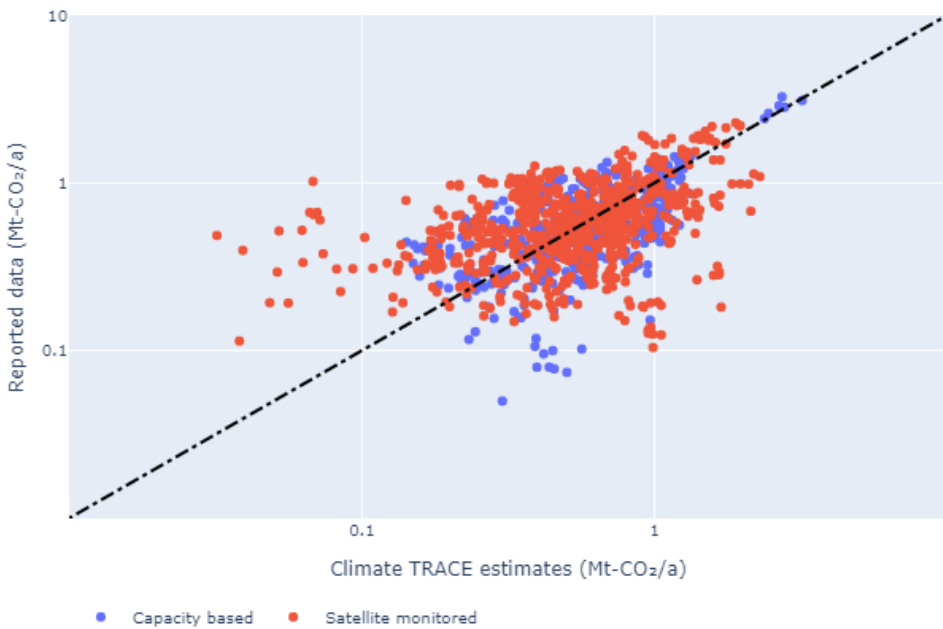


Figure 5 Comparison of asset level emissions satellite-based estimates (red dots) and capacity-based estimates (blue dots) to reported estimates from the US-EPA and E-PRTR for periods January 2015 to December 2021.

3.2. Aggregated emissions estimates for EU, US

Asset level emissions estimates are the target of this work. However, it is also useful to validate our results at a more aggregated level. Figure 6 highlights the results based on aggregated annually reported emissions for selected plants (as stated in Section 3.2) in the EU and US, respectively. In both cases data is compared as aggregate values across years 2015 to 2020 and our own estimates demonstrate high levels of accuracy to reported data. For the EU a MAE (MAPE) of 1.8 Mt/a (3%) and the US a 1.1 Mt/a (2%) is achieved. It should be noted that the number of assets compared each year is listed in brackets.

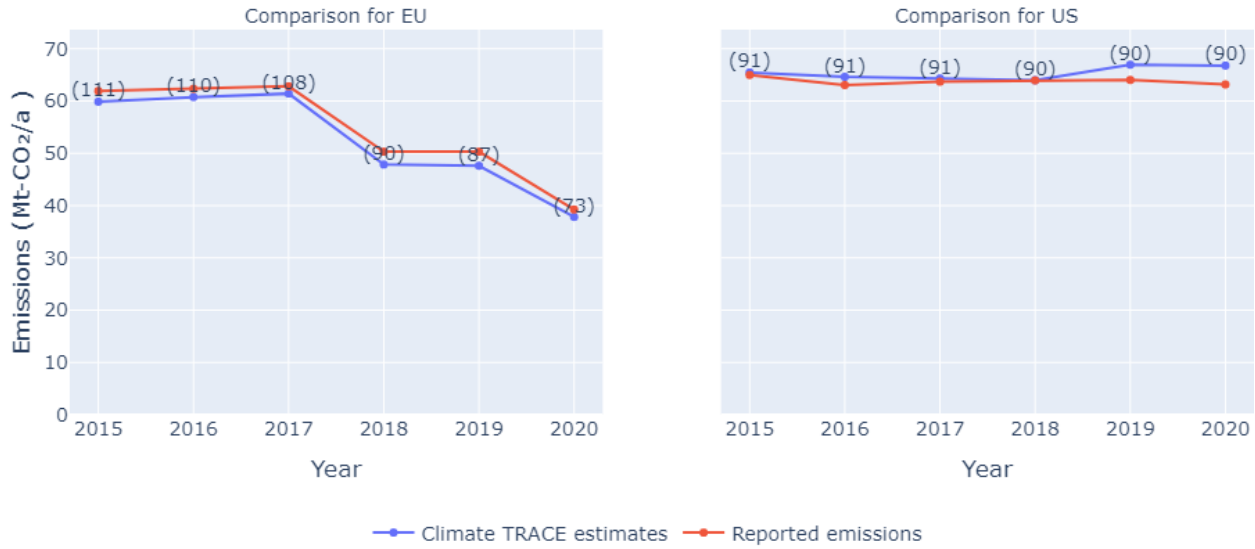


Figure 6 Comparison of reported emissions and Climate TRACE emissions estimates for the EU (left) and US (right). Number of available assets for each comparison shown in brackets.

4. Discussion

Our cement emissions estimates modelling approach consists of first, estimating facility level production, and second, applying a relevant emissions factor to yield facility emissions. The approach for estimating cement production at the facility level is dependent upon availability of data. For 52% (1178 out of 2256) of our assets a satellite-based monitoring approach is used. For the remaining 48% of assets, the capacity-based approach is used. Satellite-based approach is ideal in that the production of each asset is estimated based on the heat activity for a given period. This allows for more representative production dynamics for an asset, such as capturing if a plant has been switched off. Capacity based assets do not demonstrate these same characteristics and instead are characterised by their capacity-based share of national production. There are several reasons for assets whose production cannot reliably be estimated using satellite images. Most often, assets are excluded from satellite monitoring due to a small signal-to-noise ratio which makes it difficult to distinguish between production and background fluctuations. Other sources of complication can be the occasional presence of strong reflections from a-priori cold elements, or the fact that kilns may be placed inside a building and hidden by a roof. A representative example is shown in Section 7.3, Figure 10. To determine which facilities are monitored by satellite, each plant is processed with an algorithm that automatically determines whether suitable hotspots exist depending on how much the NHI varies as a function of time within predefined regions containing hot pixels. An acceptance criterion based on this noise is used to make the final decision. Currently approximately half the assets are included in satellite-based monitoring, however improvements could likely be made here through further experimentation with the acceptance criterion. The overall accuracy for the capacity and satellite monitored assets was similar at 0.20 MtCO₂/a (31%) and 0.22 MtCO₂/a (33%), respectively,

highlighting little accuracy advantage for satellite-based monitoring at this current stage (beneficial still in that country level production is not required for future estimates). Current limitations arise from the satellite model optimiser which has a tendency to overestimate some assets and underestimate others when weakly constrained. Ultimately this results in good accuracy results at the aggregate (i.e., country) level results, as seen in Figure 6 for EU and US, at the expense of poorer asset level results. One approach to address this problem is to add more constraints at the asset level (such as knowledge of production values for a single month or year) which could assist in tuning each country's model. This prospect will be one of the focusses of future iterations on this work.

In some cases, inaccuracies in our own emissions estimates may be due to factors less within our control. Three main hypotheses are presented for differences in emissions estimates: (1) different reporting scope, (2) country/region specific emissions factors, (3) limitations in the asset database, and there could additionally be many causes for these discrepancies for which it is not always trivial to identify in each facility. A difference in reporting scope of the emissions between the reported data and the emission factors is suspected in some cases. In our own models we look to compare direct emissions, however, reported values were not always clear on their exact scope. An example may be that two facilities might report their associated electricity emissions differently (depending on the availability or absence of on-site power generation), making it harder to consistently compare reported data with our direct emissions estimates. Another reason can be linked to the fact that the emission factors we use are country/region and production method specific. For countries with numerous facilities these values may not always be representative for each plant. Emissions intensity is likely to vary substantially based upon the age of the facility, fuel mix, feedstocks, use of energy-efficient technologies, clinker-to-cement ratio and variable share of supplementary cementitious materials added to the cement mix. Additionally, our asset database provider, Spatial Finance Initiative (SFI), provides the official capacities of 1479 out of the 2256 assets (McCarten et al., 2021). For the remaining 777 assets either geographical ($n=727$) or global mean asset production capacity values are used. Following these assumptions SFI stated capacities represent 70% of total production capacity, while 30% is that of geographical or global mean estimates.

Lastly, we wish to emphasise that the external power emissions estimated in this work include emissions originating from the grinding process, which may or may not occur in the same facility where the clinker was produced. Indeed, the SFI database contains 842 assets that are not included in the present work and that represent grinding plants, where no clinker is produced, which contribute to 23% of global cement capacity (1,260 Mt/y). In the following, power-related grinding emissions are treated as if they were occurring in the facility that produced the clinker that is to be grinded. This assumption allows us to cover a broader scope of emissions in the cement sector, but does not create a large bias on the asset-level estimate since the power-related

grinding emission factor contributes less than 5% of the total in the extreme cases (Shen *et al.*, 2014), and can be much less.

5. Conclusion

In this work a new approach has been implemented to estimate cement emissions using clinker production estimates at a facility level and monthly for 2256 integrated cement plant assets, covering 136 countries, in the SFI database. In total, based on 2021 numbers, these assets cover 75% (2,306 out of 3,063 Mt/a) of worldwide clinker production.

The clinker production was estimated using a hybrid approach of satellite-derived NHI measurements and capacity-based techniques. Where possible, satellite-based estimates allowed for the use of machine learning to infer a relationship between facility hotspots and clinker production - ultimately resulting in more granular and timely estimates. For facilities where no suitable hotspot signals could be extracted, the capacity-based approach was used to infer production estimates. Based on the 2021 production numbers, our satellite-monitored assets contribute 54% of the total asset CO₂ emissions (1,097 out of 2,022 MtCO₂/a).

To calculate emissions, country or region and process-specific (wet or dry) emission factors were applied, derived from the GNR datasets, to the estimated clinker production at a facility level. This process allowed for direct comparisons of our own models with reported emissions figures by the US EPA and E-PRTR (US EPA, 2022; E-PRTR, 2022). This process highlights the strength of our modelling in its accurate estimation of aggregated annual EU and US cement emissions, with MAE (MAPE) values 1.8 Mt/a (3%) and 1.1 Mt/a (2%) achieved, respectively. Performance at the asset level however was not as strong with an overall accuracy of 0.21 Mt/a (33%). Despite the asset level results, this work serves as a strong baseline for future work with the foundation and methodology established for satellite-based production approaches. Low-hanging fruit for easy gains in accuracy could be achieved through the introduction of further asset level constraints on top of establishing a maximum production capacity. One such promising concept is utilising a subset of facility level clinker production values used once during the initial training process - however these are more challenging to access compared to country level statistics.

Ultimately, this work has shown that timely and accurate facility level production and emissions can be obtained without the need to rely upon systematic and exhaustive factory published figures, often years out of date where these are available. Additionally, this work may open pathways to assist in future climate policy. Future work may benefit from greater availability of asset data for model training, allowing subsequent versions of our model to benefit from a greater scope of historical data that may further improve our model results. An additional source of improvement would be the inclusion of grinding plants from the SFI database to correctly

distribute cement grinding emissions, but this requires the knowledge of clinker flows between plants which has not been investigated in the scope of this work.

6. References

1. Andrew, R. (2022) ‘Cement emissions data retrieved from: Global CO₂ emissions from cement production’. Zenodo. Available at: <https://doi.org/10.5281/zenodo.6553090>.
2. Andrew, R.M. (2018) ‘Global CO₂ emissions from cement production’, *Earth System Science Data*, 10(1), pp. 195–217. Available at: <https://doi.org/10.5194/essd-11-1675-2019>.
3. Andrew, R.M. (2019) *Global CO₂ from cement production, 1928–2018*. preprint. Antroposphere - Energy and Emissions. Available at: <https://doi.org/10.5194/essd-2019-152>.
4. Construction Cost, contributors (2016) *Cement Production Process, Cement Production Process*. Available at: <https://www.constructioncost.co/cement-production-process.html> (Accessed: 31 August 2022).
5. E-PRTR contributors (2022) ‘Cement emissions data retrieved from: E-PRTR’. European Pollutant Release and Transfer Register (E-PRTR). Available at: <http://prtr.ec.europa.eu/>.
6. European Space Agency (ESA) (2022) ‘Satellite images data retrieved from: Copernicus Sentinel-2 ESA’. Available at: https://www.esa.int/Applications/Observing_the_Earth/Copernicus/Sentinel-2.
7. GNR contributors (2020) ‘Cement emission factor data retrieved from: GCCA Getting the Numbers Right’. Global Cement and Concrete Association (GCCA). Available at: <https://gcccassociation.org/gnr/> (Accessed: 15 July 2022).
8. Google Earth Engine (2022a) *Landsat 8 Datasets in Earth Engine*, Google Developers. Available at: <https://developers.google.com/earth-engine/datasets/catalog/landsat-8> (Accessed: 26 July 2022).
9. Google Earth Engine (2022b) *Landsat 9 Datasets in Earth Engine*, Google Developers. Available at: <https://developers.google.com/earth-engine/datasets/catalog/landsat-9> (Accessed: 26 July 2022).
10. Google Earth Engine (2022c) *Sentinel-2 Datasets in Earth Engine*, Google Developers. Available at: <https://developers.google.com/earth-engine/datasets/catalog/sentinel-2> (Accessed: 26 July 2022).
11. Google Maps contributors (2022) ‘Cement inventory data retrieved from: Google Maps’. Google. Available at: <https://www.google.co.uk/maps>.
12. IEA (2018) ‘Technology Roadmap - Low-Carbon Transition in the Cement Industry’, *International Energy Agency (IEA)*, p. 66.
13. IEA (2020) ‘Power grid intensities data retrieved from: IEA Global Energy Review 2020’. International Energy Agency (IEA). Available at: <https://www.iea.org/reports/global-energy-review-2020> (Accessed: 26 August 2022).
14. IPCC (2006) ‘Cement emission factor data retrieved from: IPCC Emission Factor Database (ID: 213926)’. Intergovernmental Panel on Climate Change (IPCC). Available at: https://www.ipcc-npp.iges.or.jp/EFDB/find_ef.php?ipcc_code=2.A.1&ipcc_level=2 (Accessed: 26 August 2022).
15. Kato, S. (2021) *Automated classification of heat sources detected using SWIR remote sensing | Elsevier Enhanced Reader*. Available at: <https://doi.org/10.1016/j.jag.2021.102491>.
16. Liangrocapart, S., Khetkeeree, S. and Petchthaweeetham, B. (2020) ‘Thermal Anomaly Level Algorithm for Active Fire Mapping by Means of Sentinel-2 Data’, in *2020 17th International Conference on Electrical Engineering/Electronics, Computer, Telecommunications and Information Technology (ECTI-CON)*. *2020 17th International Conference on Electrical Engineering/Electronics, Computer, Telecommunications and Information Technology*

- (*ECTI-CON*), pp. 687–690. Available at: <https://doi.org/10.1109/ECTI-CON49241.2020.9158262>.
17. Marchese, F. *et al.* (2019) ‘A Multi-Channel Algorithm for Mapping Volcanic Thermal Anomalies by Means of Sentinel-2 MSI and Landsat-8 OLI Data’, *Remote Sensing*, 11(23), p. 2876. Available at: <https://doi.org/10.3390/rs11232876>.
 18. M’Barek, B. and Gray, M. (2021) ‘The Spotlight Effect’. Transition Zero. Available at: <https://www.transitionzero.org/reports/the-spotlight-effect>.
 19. MBS (2022) ‘Cement production data retrieved from: UNdata Monthly Bulletin of Statistics Online’. UNdata. Available at: https://unstats.un.org/unsd/mbs/table_list.aspx (Accessed: 26 August 2022).
 20. National Aeronautics and Space Administration (NASA) (2018) ‘Band Pass Adjustment’. Available at: <https://hls.gsfc.nasa.gov/algorithms/bandpass-adjustment/> (Accessed: 25 July 2022).
 21. National Aeronautics and Space Administration (NASA) and United States Geological Survey (USGS) (2022a) ‘Satellite images data retrieved from: Landsat-8 NASA/USGS’. Available at: <https://www.usgs.gov/landsat-missions/landsat-8>.
 22. National Aeronautics and Space Administration (NASA) and United States Geological Survey (USGS) (2022b) ‘Satellite images data retrieved from: Landsat-9 NASA/USGS’. Available at: <https://www.usgs.gov/landsat-missions/landsat-9>.
 23. OpenStreetMap contributors (2022) ‘Cement inventory data retrieved from: OpenStreetMap’. OpenStreetMap. Available at: <https://www.openstreetmap.org/>.
 24. McCarten, M., Bayaraa, M., Caldecott, B., Christiaen, C., Foster, P., Hickey, C., Kampmann, D., Layman, C., Rossi, C., Scott, K., Tang, K., Tkachenko, N., and Yoken, D. (2021). Global Database of Iron and Steel Production Assets. Spatial Finance Initiative. Available at: <https://www.cfgi.ac.uk/spatial-finance-initiative/geoasset-project/geoasset-databases/> (Accessed: 26 August 2022).
 25. Shen, L. *et al.* (2014) ‘Factory-level measurements on CO₂ emission factors of cement production in China’, *Renewable and Sustainable Energy Reviews*, 34, pp. 337–349. Available at: <https://doi.org/10.1016/j.rser.2014.03.025>.
 26. UN Comtrade (2022) ‘Clinker imports data retrieved from: UN Comtrade’. United Nations. Available at: <https://comtrade.un.org/data/> (Accessed: 30 August 2022).
 27. UNFCCC contributors (2022) ‘Cement emissions data retrieved from: UNFCCC’. United Nations Framework Convention on Climate Change (UNFCCC). Available at: <https://unfccc.int/process-and-meetings/transparency-and-reporting/greenhouse-gas-data/ghg-data-unfccc/ghg-data-from-unfccc>.
 28. UNIDO (2022) ‘Non-metallic mineral production data retrieved from: UNIDO’. United Nations Industrial Development Organization (UNIDO). Available at: <https://stat.unido.org/database/Monthly%20IIP> (Accessed: 26 August 2022).
 29. US EPA contributors (2022) ‘Cement emissions data retrieved from: US EPA’. United States Environmental Protection Agency (US EPA). Available at: <https://www.epa.gov/>.
 30. USGS (2022) ‘Cement production data retrieved from: USGS Cement Statistics and Information’. U.S. Geological Survey (USGS). Available at: <https://www.usgs.gov/centers/national-minerals-information-center/cement-statistics-and-information> (Accessed: 26 August 2022).
 31. Zhou, Y. *et al.* (2018) ‘A Method for Monitoring Iron and Steel Factory Economic Activity Based on Satellites’, *Sustainability*, 10(6), p. 1935. Available at:

7. Appendices

7.1. Overview of the cement production process

The cement production process starts with mining and quarrying, where raw materials are extracted from the environment. Then, three main operations are performed. First, raw meals made of an appropriate mix of crushed limestone, calcium, silicon, aluminium and iron oxides are prepared. Second, raw meals are placed into a kiln where a large flame elevates the temperature greatly to allow for formation of clinker by chemical reaction and thereby releasing CO₂. The thermal energy provided by the kiln originates from the combustion of various types of fuels ranging from traditional fossil fuels like coal and oil to alternative waste fuels and biomass. Third, cooled clinkers are ground and mixed with gypsum to create cement. An overview of this process is highlighted in Figure 7.

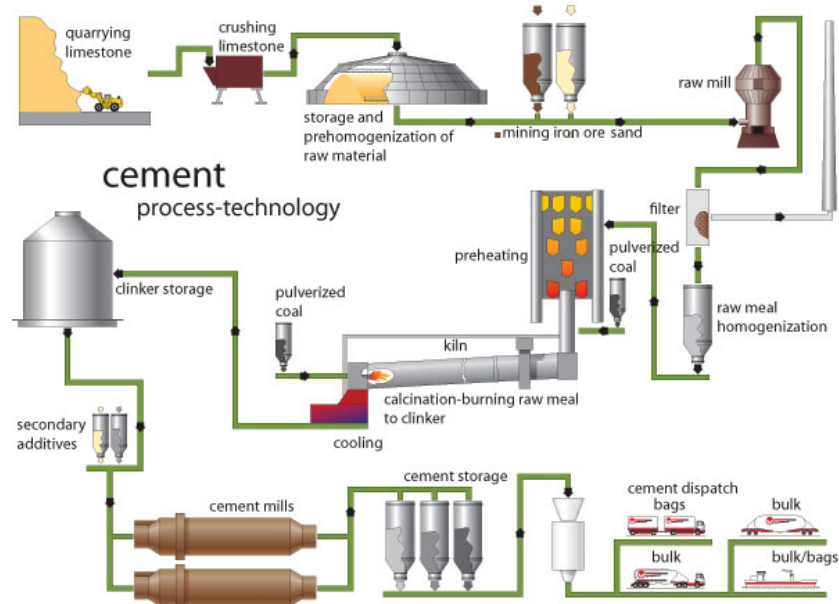


Figure 7 Overview of the cement production process (Construction Cost, contributors, 2016).

7.2. Extracting clinker production

Monthly clinker production is estimated in two steps. First, the cement production is directly retrieved or estimated depending on data availability. Then, it is converted to clinker using a cement-to-clinker ratio and subtracting cement imports. These two steps are detailed below.

7.2.1. Extracting cement production

To extract cement production, four models were developed, which were defined by the requisite data available.

- Model (1), the preferred option, which consists in directly retrieving country reported clinker production statistics. This was only possible for a select few countries: United states (at state level) and, China (at province level), and Japan (at country level).
- Model (2) uses MBS and USGS data. MBS provides reported figures from January 2009 to June 2018 while UNIDO data reports the monthly non-metallic mineral production index. By following the assumption that cement production and non-metallic mineral production have a proportional seasonal relationship, and knowledge of total annual cement production available through USGS, a model is trained against MBS data to infer the most recent (>June 2018) cement production data.
- Model (3) utilises UNIDO data trained against USGS data to yield estimates that still capture the seasonal pattern of cement production.
- Model (4) uses only the USGS annual data and assumes constant production throughout the year.

In total the four models were applied in the following ways: Model (1) - 51 geographies (China, 31 provinces; US, 19 state-collections which are subsets of US states defined in USGS reported data) and total capacity of 1,748 Mt/a (43% monitored global capacity), Model (2) - 31 geographies and total capacity of 738 Mt/a (18%), Model (3) - 37 geographies and total capacity 861 Mt/a (21%), and Model (4) - 151 geographies and total capacity 747 Mt/a (18%). Figure 8 demonstrates each of these approaches relative to the reported cement production of the United States.



Figure 8 A comparison of the United States monthly cement production data obtained from the 4 models defined in this section.

7.2.1. Inferring clinker production from cement production

Given the cement production inferred from our modelling, the goal was to derive the volume of clinker produced for a given geography given a known cement-to-clinker ratio while also accounting for net imports of clinker. This relationship is denoted by,

$$P_k = P_c / \alpha - N_{ik}$$

where P_k is the desired output, production of clinker, P_c is the known production of cement, α is the ratio of cement to clinker, and N_{ik} quantifies the net imports of clinker retrieved from the UN Comtrade database. The parameter α is estimated on the country level based on the average of the previous 5 years of production and emissions data through the following,

$$\begin{aligned} (1) \quad & E = P_k e_k \\ (2) \quad & P_c = D_k \alpha = (P_k + N_{ik}) \alpha = (E/e_k + N_{ik}) \alpha \\ (3) \quad & \alpha = P_c / (E/e_k + N_{ik}) \end{aligned}$$

where E is the reported emissions associated with cement production process retrieved from¹ (Andrew, 2022), e_k is the known emission factor associated with clinker production (see Section 2.2.2) and D_k the demand for clinker. An example of this process is shown for the US in Figure 9 whereby reported cement production was combined with known trading data, emissions data, and cement to clinker emissions factor to produce a clinker production estimate. These values were subsequently compared to reported clinker production figures by USGS.

¹ The reference itself is heavily based on emissions reported by the United Nations Framework Convention on Climate Change (UNFCCC contributors, 2022).

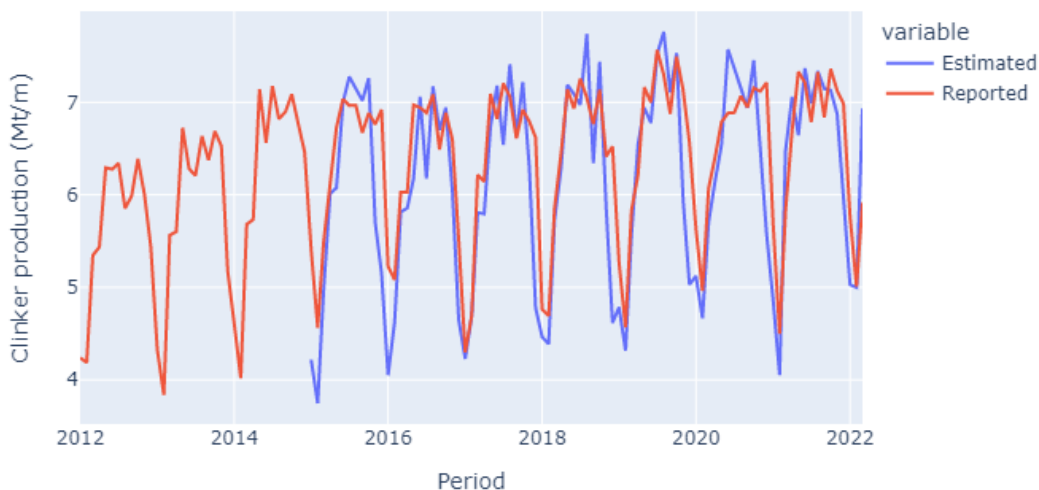


Figure 9 A comparison of the United States monthly clinker production reported values versus our own estimated value.

7.3. Limits to hotspot mapping

Figure 10 depicts an example of a cement plant that is not monitored with satellite due to small signal-to-noise ratio limitations discussed in Section 4. Not only the heat signal is much more diluted around the kiln in comparison to the plant of Figure 2, but we also observe undesired signals originating from reflections on the coal stack.



Figure 10 Left - High resolution image of the Stockertown cement plant in Pennsylvania, United States. Right - composite Sentinel-2 image of the same plant. Heat signals (red areas) are not situated over kiln areas but on the coal stack. Sources: modified Copernicus and USGS data.

7.4. Summary of the coverage by geographies (2021)

Table 3 Summary of the data coverage by country, with a breakdown of the cement plants monitored by satellite (expressed by number of assets, share of installed capacity, production and emissions). Values representative for 2021.

Country	Total assets	Satellite-monitored assets	Total asset production (Mt clinker)	Satellite-monitored production (Mt clinker)	Total assets emissions (MtCO2)	Satellite-monitored emissions (MtCO2)
China	909	534 (59%)	927.6	569.2 (61%)	807.3	495.4 (61%)
India	151	50 (33%)	258.8	89.4 (35%)	229.2	79.2 (35%)
Vietnam	50	26 (52%)	81.0	45.5 (56%)	71.8	40.3 (56%)
United States	91	37 (41%)	75.0	30.5 (41%)	67.9	27.7 (41%)
Indonesia	22	3 (14%)	50.8	4.53 (9%)	45.0	4.02 (9%)
Brazil	59	18 (31%)	48.1	12.8 (27%)	38.9	10.4 (27%)
Saudi Arabia	18	11 (61%)	46.9	32.0 (68%)	41.8	28.5 (68%)
Turkey	54	49 (91%)	46.2	37.8 (82%)	41.1	33.6 (82%)
Russia	50	45 (90%)	42.4	39.4 (93%)	40.8	37.6 (92%)
South Korea	12	10 (83%)	42.3	37.2 (88%)	36.8	32.3 (88%)
Iran	69	36 (52%)	38.7	20.2 (52%)	34.5	18.0 (52%)
Mexico	33	23 (70%)	38.5	23.1 (60%)	35.0	21.0 (60%)
Japan	31	27 (87%)	38.2	35.5 (93%)	33.3	30.9 (93%)
Pakistan	29	18 (62%)	36.3	22.6 (62%)	32.2	20.1 (62%)
Thailand	11	3 (27%)	35.5	12.3 (35%)	30.1	10.4 (35%)
Egypt	24	12 (50%)	27.1	14.9 (55%)	24.9	13.6 (55%)
Germany	30	0 (0.0%)	25.9	0.00 (0.0%)	21.6	0.00 (0.0%)
Philippines	15	5 (33%)	19.5	10.2 (53%)	18.2	9.60 (53%)
Algeria	16	15 (94%)	18.9	18.8 (99%)	15.8	15.7 (99%)
Spain	29	17 (59%)	17.0	11.0 (65%)	13.9	9.01 (65%)

Nigeria	10	4 (40%)	16.7	3.00 (18%)	14.9	2.67 (18%)
Italy	35	11 (31%)	16.3	4.86 (30%)	14.0	4.17 (30%)
Malaysia	9	1 (11%)	15.6	2.71 (17%)	13.9	2.41 (17%)
Canada	16	9 (56%)	12.9	9.55 (74%)	10.7	7.91 (74%)
France	28	16 (57%)	12.7	6.51 (51%)	10.4	5.34 (51%)
Colombia	15	4 (27%)	11.7	3.48 (30%)	10.0	3.12 (31%)
Poland	10	7 (70%)	10.50	8.44 (80%)	9.29	7.44 (80%)
Iraq	16	0 (0.0%)	10.20	0.00 (0.0%)	9.43	0.00 (0.0%)
South Africa	13	9 (69%)	9.72	6.12 (63%)	8.64	5.44 (63%)
Nepal	8	0 (0.0%)	9.29	0.00 (0.0%)	8.24	0.00 (0.0%)
Argentina	15	9 (60%)	9.14	6.40 (70%)	7.68	5.38 (70%)
Ukraine	11	7 (64%)	8.60	4.97 (58%)	7.73	4.34 (56%)
Uzbekistan	6	3 (50%)	8.25	6.07 (74%)	7.68	5.78 (75%)
Peru	6	4 (67%)	7.96	5.44 (68%)	6.69	4.57 (68%)
Morocco	12	9 (75%)	7.93	6.77 (85%)	6.80	5.80 (85%)
United Kingdom	12	6 (50%)	7.80	4.88 (63%)	6.61	4.23 (64%)
Kazakhstan	10	0 (0.0%)	7.57	0.00 (0.0%)	6.88	0.00 (0.0%)
Ethiopia	7	3 (43%)	7.44	2.61 (35%)	6.61	2.32 (35%)
Romania	6	6 (100%)	7.27	7.27 (100%)	6.03	6.03 (100%)
United Arab Emirates	13	9 (69%)	7.07	6.64 (94%)	6.29	5.91 (94%)
Cambodia	5	3 (60%)	6.61	4.79 (72%)	5.86	4.24 (72%)
Taiwan	6	0 (0.0%)	6.04	0.00 (0.0%)	5.35	0.00 (0.0%)
Myanmar	9	1 (11%)	5.74	0.86 (15%)	5.22	0.76 (15%)
Greece	6	0 (0.0%)	5.60	0.00 (0.0%)	4.64	0.00 (0.0%)
Tunisia	8	6 (75%)	5.03	3.82 (76%)	4.19	3.19 (76%)

Tanzania	6	4 (67%)	4.93	2.89 (59%)	4.38	2.57 (59%)
Kenya	4	0 (0.0%)	4.89	0.00 (0.0%)	4.35	0.00 (0.0%)
Belgium	4	4 (100%)	4.79	4.79 (100%)	4.31	4.31 (100%)
Laos	6	1 (17%)	4.12	0.81 (20%)	3.65	0.72 (20%)
Dominican Republic	5	0 (0.0%)	4.02	0.00 (0.0%)	3.65	0.00 (0.0%)
Czech Republic	4	4 (100%)	3.71	3.71 (100%)	3.09	3.09 (100%)
Ireland	4	4 (100%)	3.66	3.66 (100%)	3.04	3.04 (100%)
Lebanon	3	0 (0.0%)	3.63	0.00 (0.0%)	3.23	0.00 (0.0%)
Australia	7	3 (43%)	3.59	1.73 (48%)	3.20	1.53 (48%)
Senegal	3	1 (33%)	3.58	1.17 (33%)	3.19	1.04 (33%)
Belarus	3	2 (67%)	3.50	3.03 (87%)	3.14	2.65 (84%)
Ecuador	4	2 (50%)	3.46	2.40 (70%)	3.14	2.18 (70%)
Portugal	6	3 (50%)	3.44	2.50 (73%)	2.85	2.08 (73%)
Austria	8	5 (62%)	3.39	2.65 (78%)	2.71	2.12 (78%)
Kuwait	2	1 (50%)	3.31	0.88 (26%)	2.96	0.78 (26%)
Oman	2	1 (50%)	3.30	1.62 (49%)	2.94	1.44 (49%)
Venezuela	10	1 (10%)	3.30	0.68 (21%)	2.91	0.68 (23%)
Qatar	2	0 (0.0%)	3.19	0.00 (0.0%)	2.84	0.00 (0.0%)
Libya	6	2 (33%)	3.10	1.19 (39%)	2.75	1.06 (39%)
Bolivia	7	3 (43%)	2.96	1.67 (56%)	2.49	1.40 (56%)
Switzerland	5	4 (80%)	2.95	2.57 (87%)	2.44	2.13 (87%)
Sudan	6	4 (67%)	2.93	1.99 (68%)	2.60	1.77 (68%)
Turkmenistan	4	0 (0.0%)	2.92	0.00 (0.0%)	2.59	0.00 (0.0%)
Guatemala	3	0 (0.0%)	2.83	0.00 (0.0%)	2.57	0.00 (0.0%)
Sweden	2	2 (100%)	2.54	2.54 (100%)	2.10	2.10 (100%)

Uganda	2	0 (0.0%)	2.46	0.00 (0.0%)	2.19	0.00 (0.0%)
Slovakia	4	3 (75%)	2.42	2.06 (85%)	2.01	1.71 (85%)
Angola	4	0 (0.0%)	2.28	0.00 (0.0%)	2.03	0.00 (0.0%)
Croatia	5	2 (40%)	2.28	0.56 (24%)	1.89	0.46 (25%)
Denmark	1	1 (100%)	2.27	2.27 (100%)	1.88	1.88 (100%)
North Korea	2	1 (50%)	2.19	1.10 (50%)	1.91	0.95 (50%)
Azerbaijan	3	3 (100%)	2.17	2.17 (100%)	1.89	1.89 (100%)
Jordan	5	2 (40%)	2.01	1.18 (59%)	1.79	1.05 (59%)
Serbia	3	2 (67%)	1.97	1.32 (67%)	1.63	1.10 (67%)
Hungary	4	2 (50%)	1.89	0.83 (44%)	1.57	0.69 (44%)
Tajikistan	1	1 (100%)	1.88	1.88 (100%)	1.96	1.96 (100%)
Bulgaria	3	3 (100%)	1.83	1.83 (100%)	1.52	1.52 (100%)
Honduras	2	0 (0.0%)	1.75	0.00 (0.0%)	1.59	0.00 (0.0%)
Zambia	6	2 (33%)	1.68	0.28 (17%)	1.49	0.25 (17%)
Georgia	2	2 (100%)	1.61	1.61 (100%)	1.50	1.50 (100%)
Cameroon	1	0 (0.0%)	1.55	0.00 (0.0%)	1.38	0.00 (0.0%)
Albania	3	2 (67%)	1.50	1.42 (95%)	1.24	1.18 (95%)
Syria	7	2 (29%)	1.40	0.40 (29%)	1.26	0.36 (28%)
Kyrgyzstan	3	2 (67%)	1.38	1.26 (91%)	1.37	1.24 (90%)
Israel	1	1 (100%)	1.36	1.36 (100%)	1.21	1.21 (100%)
Costa Rica	2	2 (100%)	1.34	1.34 (100%)	1.22	1.22 (100%)
Yemen	6	2 (33%)	1.32	0.54 (41%)	1.17	0.48 (41%)
Cyprus	1	1 (100%)	1.31	1.31 (100%)	1.09	1.09 (100%)
Bahrain	1	0 (0.0%)	1.24	0.00 (0.0%)	1.10	0.00 (0.0%)
Moldova	1	1 (100%)	1.24	1.24 (100%)	1.08	1.08 (100%)

Cuba	4	2 (50%)	1.13	0.64 (57%)	1.05	0.58 (55%)
Lithuania	1	1 (100%)	1.11	1.11 (100%)	0.92	0.92 (100%)
Zimbabwe	4	0 (0.0%)	1.09	0.00 (0.0%)	0.97	0.00 (0.0%)
Finland	2	2 (100%)	1.09	1.09 (100%)	0.90	0.90 (100%)
Mongolia	3	1 (33%)	1.08	0.36 (34%)	0.94	0.32 (34%)
Panama	1	1 (100%)	1.08	1.08 (100%)	0.98	0.98 (100%)
Latvia	1	1 (100%)	1.05	1.05 (100%)	0.87	0.87 (100%)
Chile	5	5 (100%)	0.93	0.93 (100%)	0.78	0.78 (100%)
Slovenia	2	0 (0.0%)	0.90	0.00 (0.0%)	0.74	0.00 (0.0%)
Namibia	2	0 (0.0%)	0.88	0.00 (0.0%)	0.78	0.00 (0.0%)
Democratic Republic of the Congo	4	0 (0.0%)	0.88	0.00 (0.0%)	0.79	0.00 (0.0%)
Bhutan	2	0 (0.0%)	0.86	0.00 (0.0%)	0.77	0.00 (0.0%)
Paraguay	2	0 (0.0%)	0.86	0.00 (0.0%)	0.73	0.00 (0.0%)
Bangladesh	1	0 (0.0%)	0.84	0.00 (0.0%)	0.75	0.00 (0.0%)
Norway	2	2 (100%)	0.76	0.76 (100%)	0.63	0.63 (100%)
El Salvador	2	0 (0.0%)	0.76	0.00 (0.0%)	0.69	0.00 (0.0%)
Armenia	2	0 (0.0%)	0.75	0.00 (0.0%)	0.72	0.00 (0.0%)
Sri Lanka	1	1 (100%)	0.75	0.75 (100%)	0.66	0.66 (100%)
Uruguay	2	1 (50%)	0.72	0.15 (21%)	0.61	0.13 (21%)
Macedonia	1	0 (0.0%)	0.66	0.00 (0.0%)	0.54	0.00 (0.0%)
New Zealand	1	0 (0.0%)	0.63	0.00 (0.0%)	0.56	0.00 (0.0%)
Jamaica	2	0 (0.0%)	0.61	0.00 (0.0%)	0.56	0.00 (0.0%)
Togo	2	1 (50%)	0.61	0.59 (97%)	0.54	0.53 (97%)
Bosnia and Herzegovina	2	1 (50%)	0.60	0.47 (79%)	0.50	0.39 (79%)

Benin	2	1 (50%)	0.60	0.20 (34%)	0.53	0.18 (34%)
Republic of Congo	3	0 (0.0%)	0.54	0.00 (0.0%)	0.48	0.00 (0.0%)
Trinidad and Tobago	1	0 (0.0%)	0.50	0.00 (0.0%)	0.42	0.00 (0.0%)
Luxembourg	1	1 (100%)	0.50	0.50 (100%)	0.42	0.42 (100%)
Gabon	1	0 (0.0%)	0.42	0.00 (0.0%)	0.44	0.00 (0.0%)
Rwanda	1	1 (100%)	0.41	0.41 (100%)	0.36	0.36 (100%)
Ghana	1	0 (0.0%)	0.30	0.00 (0.0%)	0.27	0.00 (0.0%)
Malawi	1	0 (0.0%)	0.26	0.00 (0.0%)	0.23	0.00 (0.0%)
Eritrea	2	0 (0.0%)	0.20	0.00 (0.0%)	0.18	0.00 (0.0%)
Niger	1	0 (0.0%)	0.20	0.00 (0.0%)	0.18	0.00 (0.0%)
Chad	1	0 (0.0%)	0.20	0.00 (0.0%)	0.18	0.00 (0.0%)
Djibouti	1	0 (0.0%)	0.14	0.00 (0.0%)	0.13	0.00 (0.0%)
Haiti	1	0 (0.0%)	0.14	0.00 (0.0%)	0.16	0.00 (0.0%)
Estonia	1	1 (100%)	0.14	0.14 (100%)	0.13	0.13 (100%)
Barbados	1	1 (100%)	0.13	0.13 (100%)	0.12	0.12 (100%)
Nicaragua	1	0 (0.0%)	0.13	0.00 (0.0%)	0.14	0.00 (0.0%)
Afghanistan	1	0 (0.0%)	0.02	0.00 (0.0%)	0.03	0.00 (0.0%)

Table 4 Summary of the coverage in Chinese provinces, with a breakdown of the cement plants monitored by satellite in the coverage (expressed by number of assets, share of installed capacity, production and emissions). Values representative for 2021.

Chinese province	Total assets	Satellite-monitored assets	Total asset production (Mt clinker)	Satellite-monitored production (Mt clinker)	Total assets emissions (MtCO2)	Satellite-monitored emissions (MtCO2)
Shandong	58	19 (33%)	72.0	20.0 (28%)	62.7	17.4 (28%)
Anhui	39	31 (79%)	58.5	55.1 (94%)	50.9	48.0 (94%)
Henan	45	17 (38%)	54.8	20.9 (38%)	47.7	18.2 (38%)
Hebei	53	34 (64%)	53.2	34.0 (64%)	46.3	29.6 (64%)
Hunan	49	28 (57%)	52.8	37.7 (71%)	46.0	32.8 (71%)
Sichuan	67	39 (58%)	52.7	26.6 (50%)	45.9	23.1 (50%)
Zhejiang	42	27 (64%)	45.4	33.8 (74%)	39.5	29.4 (74%)
Hubei	37	22 (59%)	43.9	30.2 (69%)	38.2	26.3 (69%)
Guangxi	32	24 (75%)	43.4	37.0 (85%)	37.8	32.2 (85%)
Yunnan	46	37 (80%)	42.4	35.6 (84%)	36.9	31.0 (84%)
Jiangxi	34	25 (74%)	40.3	27.0 (67%)	35.0	23.5 (67%)
Guangdong	31	25 (81%)	34.0	28.6 (84%)	29.6	24.9 (84%)
Guizhou	49	29 (59%)	33.6	15.1 (45%)	29.3	13.1 (45%)
Shaanxi	35	24 (69%)	32.2	24.8 (77%)	28.0	21.6 (77%)
Jiangsu	23	15 (65%)	30.9	21.9 (71%)	26.9	19.0 (71%)
Shanxi	35	13 (37%)	30.3	10.3 (34%)	26.4	8.97 (34%)
Inner Mongolia	30	16 (53%)	29.0	13.7 (47%)	25.2	11.9 (47%)
Xinjiang	38	10 (26%)	26.1	5.98 (23%)	22.7	5.20 (23%)
Liaoning	28	17 (61%)	25.6	16.5 (64%)	22.3	14.3 (64%)
Fujian	26	18 (69%)	25.2	19.2 (76%)	21.9	16.7 (76%)
Gansu	27	10 (37%)	23.9	9.17 (38%)	20.8	7.98 (38%)

Heilongjiang	12	4 (33%)	15.3	5.16 (34%)	13.3	4.49 (34%)
Chongqing	26	22 (85%)	15.2	11.3 (74%)	13.2	9.79 (74%)
Jilin	15	9 (60%)	14.8	9.27 (63%)	12.9	8.07 (63%)
Ningxia	11	10 (91%)	9.6	9.12 (96%)	8.3	7.94 (96%)
Qinghai	8	4 (50%)	7.4	4.30 (58%)	6.4	3.74 (58%)
Beijing	7	1 (14%)	7.09	1.25 (18%)	6.17	1.09 (18%)
Hainan	3	1 (33%)	4.24	1.75 (41%)	3.69	1.52 (41%)
Tibet	2	2 (100%)	2.91	2.91 (100%)	2.54	2.54 (100%)
Tianjin	1	1 (100%)	1.00	1.00 (100%)	0.87	0.87 (100%)